

Rotational quenching of rotationally-excited H₂O in collisions with He

Benhui Yang¹, M. Nagao², W. Satomi², M. Kimura^{2,3}, and P. C. Stancil¹

Received _____; accepted _____

Resubmitted October 31, 2019 to the *Astrophysical Journal*

¹Department of Physics and Astronomy and the Center for Simulational Physics, The University of Georgia, Athens, GA 30602; yang@physast.uga.edu, stancil@physast.uga.edu

²Graduate School of Sciences, Kyushu University, Fukuoka 812-8581, Japan

³Deceased

ABSTRACT

Theoretical rotational quenching cross sections and rate coefficients of ortho- and para-H₂O due to collisions with He atoms are presented. The complete angular momentum close-coupling approach as well as the coupled-states approximation for angular momentum decoupling were applied to solve the scattering problem for a large range of rotationally-excited states of water. Results are obtained for quenching from initial levels $1_{1,0}$, $2_{1,2}$, $2_{2,1}$, $3_{0,3}$, $3_{1,2}$, $3_{2,1}$, $4_{1,4}$, $3_{3,0}$, and $4_{2,3}$ of ortho-H₂O and from initial levels $1_{1,1}$, $2_{0,2}$, $2_{1,1}$, $2_{2,0}$, $3_{1,3}$, $3_{2,2}$, $4_{0,4}$, $4_{1,3}$, and $3_{3,1}$ of para-H₂O for kinetic energies from 10^{-5} to 10^4 cm⁻¹. State-to-state and total deexcitation cross sections and rate coefficients for temperatures between 0.1 and 3000 K are reported. The present state-to-state rate coefficients are found to be in good agreement with previous results obtained by Green and coworkers at high temperatures, but significant discrepancies are obtained at lower temperatures likely due to differences in the adopted potential energy surfaces. Astrophysical applications of the current rate coefficients are briefly discussed.

Subject headings: molecular processes — molecular data — ISM: molecules

1. INTRODUCTION

Water is one of the most important molecules in a large variety of astrophysical environments. As such it is the focus of a Key program for the *Herschel Space Observatory*, Water In Star-forming regions with *Herschel* (WISH). WISH is designed to probe the physical and chemical structures of young stellar objects using water and related molecules and to follow the water abundance from collapsing clouds to planet-forming disks (van Dishoeck et al. 2011). Water has been detected in observations with *Herschel* in the massive star-forming region W3 IRS5 (Chavarría et al. 2010), in dark regions (Caselli et al. 2011), and in protoplanetary disks (Carr & Najita 2008; Salyk et al. 2011), for example. Water was also detected in earlier observations by the *Submillimeter Wave Astronomy Satellite (SWAS)*, the *Infrared Space Observatory (ISO)*, *Odin*, and the *Spitzer Space Telescope*. For example, *SWAS* observed the 1_{10} - 1_{01} 556.936 GHz transition of ortho-water, which revealed the presence of widespread emission and absorption by water vapor around the strong submillimeter continuum source Sagittarius B2 (Neufeld et al. 2003). Detections of thermal water vapor absorption lines were made toward Orion IRc2 using the Short Wavelength Spectrometer (SWS) on board *ISO* (Wright et al. 2000). Franklin et al. (2008) presented detections of the 1_{10} - 1_{01} line in 18 molecular outflows with *SWAS*, while *Spitzer* presented the first clear signature of water vapor on a hot, gas planet outside our solar system, HD 189733b (Grillmair et al. 2008). A large number of H₂O lines were also observed with *Spitzer* from the outflow of NGC 2071 (Melnick et al. 2008) and studied with shock models by Flower & Pineau des Forêts (2010).

The significance of water arises primary due to its importance as a coolant (e.g., Doty & Neufeld 1997), but it is also responsible for observed maser action. Water observations serve as an important tool for studying long-sought details of the planet formation process (Ehrenreich et al. 2007). It is the most abundant molecule frozen on

grain surfaces and is found to change the optical properties of grains and to aid in the coagulation process that ultimately produces planets (Whittet et al. 2001).

To interpret observations of water emission lines, accurate line frequencies and oscillator strengths are needed, but also key are the availability and accuracy of collisional rate coefficients. Collisional state-to-state rate coefficients are of great importance to describe energy exchange processes responsible for thermal balance and line formation, particularly in low-density gas. In such situations, the molecular level populations may be out of equilibrium or driven to non-local thermodynamic equilibrium (NLTE) via external energy sources.

Most studies of collisional excitation begin with the consideration of He impact as the resulting collisional complex is weakly bound and of lower dimensionality. As such, the H₂O-He collisional system has been investigated in a number of experimental (Bickes et al. 1975; Slankas et al. 1979; Brudermann et al. 2002; Cappelletti et al. 2005; Aquillanti et al. 2005; Dick et al. 2010; Yang et al. 2010a,b) and theoretical (Green 1980; Palma et al. 1988a,b; Green 1989; Green et al. 1991; Maluendes et al. 1992; Green et al. 1993; Tao et al. 1996; Kukawska-Tarnawska et al. 1993; Calderoni et al. 2003; Hodges et al. 2002; Patkowski et al. 2002; Yang & Stancil 2007; Makarewicz 2008; Dagdigian & Alexander 2010) studies. For numerical astrophysical models, quantitative determinations of state-to-state rate coefficients for collisions of water are crucial.

As direct measurements of collisional rate coefficients are generally difficult, numerical models often rely on calculations. However, other types of measurements can be performed to give some insight to the process and the reliability of calculations. For example, pressure broadening of five transitions of water due to helium and molecular hydrogen was investigated for temperatures relevant to the cold interstellar medium by Dick et al. (2010). In the case of He, they found a significant temperature dependence which is in agreement

with results deduced from previous theoretical inelastic studies. The situation for H_2 is less satisfactory and requires further study both experimentally and theoretically (see, for example, van der Tak 2011).

Recently, state-to-state differential cross section (DCS) measurements have been performed for rotational excitation of water by He and H_2 (Yang et al. 2010a,b). The experimental data were compared to DCS calculations obtained with the close-coupling method using the potential energy surfaces (PESs) for H_2O -He (Hodges et al. 2002) and H_2O - H_2 (Faure et al. 2005; Valiron et al. 2008). Very good agreement was found for most transitions providing some confidence in the reliability of the adopted PESs.

Four PESs (Calderoni et al. 2003; Hodges et al. 2002; Patkowski et al. 2002; Makarewicz 2008) have been developed recently for the H_2O -He complex. The potentials of Hodges et al. (2002) and Patkowski et al. (2002) were constructed using symmetry-adapted perturbation theory (SAPT), referred to as SAPT-H and SAPT-P, respectively. Calderoni et al. (2003) reported their potential based on valence bond (VB) calculations. Detailed comparison of the dynamic performance on the first three potentials, SAPT-H, SAPT-P, and VB, was performed by Yang & Stancil (2007), who concluded that the SAPT-P potential (Patkowski et al. 2002) was likely the most reliable. The PES of Makarewicz (2008) is expected to be of a similar quality, but has not been adopted in scattering calculations to the best of our knowledge.

In this work, we extend the previous rotational quenching calculations of Yang & Stancil (2007) to higher levels of rotational excitation primarily utilizing the SAPT-P (Patkowski et al. 2002) PES for both para- and ortho-water. H_2O -He rate coefficients are presented for a large range of temperature which will be applicable to modeling a wide variety of astrophysical and atmospheric environments.

2. THEORETICAL METHOD

The theory for scattering of an asymmetric top, such as H₂O, with a spherical atom can be found in Garrison et al. (1976) and Green (1976). The center of the coordinate system is fixed at the center of mass of H₂O. The water molecule is located in the $x - z$ plane, with oxygen on the positive z -axis. H₂O is taken to be rigid with the O-H bonds and H-O-H angle fixed at their equilibrium positions. The interaction then depends only on the position of the He atom which is described in the usual polar coordinates: R , θ , and ϕ . For the scattering calculations, it is convenient to expand the angle dependence of the potential V in spherical harmonics $Y_{\lambda\mu}(\theta, \phi)$ as:

$$V(R, \theta, \phi) = \sum_{\lambda\mu} v_{\lambda\mu}(R)(1 + \delta_{\mu 0})^{-1}[Y_{\lambda\mu}(\theta, \phi) + (-1)^\mu Y_{\lambda, -\mu}(\theta, \phi)]. \quad (1)$$

Owing to the C_{2v} symmetry of water, only even values of μ enter the expansion. The rotational levels of H₂O are labeled by $j_{k_{-1}, k_{+1}}$, where k_{-1} and k_{+1} are the k quantum numbers in the prolate and oblate limits. Rotational wave functions were obtained by diagonalizing the rigid-rotor Hamiltonian using rotational constants, $A = 27.881 \text{ cm}^{-1}$, $B = 14.522 \text{ cm}^{-1}$, and $C = 9.278 \text{ cm}^{-1}$, with rotational energy levels taken from Kyrö (1981) and Lanquetin et al. (1999). Energy levels of the first 12 rotational states of ortho- and para-H₂O are given in Table 1.

The calculations presented in this paper were performed by applying the close-coupling (CC) approach and the coupled-states (CS) approximation (see, for example, Flower 2007) and using the SAPT-P PES, except where noted. The CC method was used to calculate rotational quenching cross sections for center-of-mass kinetic energies from 10^{-5} to 450 cm^{-1} , while the CS approximation was used from 500 to $10,000 \text{ cm}^{-1}$. All the CC and CS calculations were performed using the nonreactive scattering code MOLSCAT (Hutson & Green 1994). In the quantum scattering calculations, the coupled-channel equations were integrated using the modified log-derivative Airy propagator of

Alexander & Manolopoulos (1987) with a variable step-size. The propagation was carried out to a maximum intermolecular separation of $R = 100 \text{ \AA}$. At each energy, a sufficient number of total angular momentum partial waves was included to ensure convergence of the cross sections. The maximum value of the total angular momentum quantum number J employed in the calculations was 140. $\vec{J} = \vec{l} + \vec{j}$ and l is the orbital angular momentum of the complex. All calculations include 5 to 10 energetically closed channels to ensure converged cross sections. As a consequence of the nuclear spins of the two hydrogen atoms in H_2O , water exists in two forms: para- H_2O and ortho- H_2O . The ortho- and para-levels do not interconvert in nonreactive collisions and are therefore treated separately in the current inelastic calculations.

The cross sections were thermally averaged over a Maxwellian kinetic energy distribution to yield state-to-state rate coefficients from specific initial rotational states $j_{k-1,k+1}$ as functions of the temperature T ,

$$k_{j_{k-1,k+1} \rightarrow j'_{k-1,k+1}}(T) = \left(\frac{8}{\pi m \beta} \right)^{1/2} \beta^2 \int_0^\infty E_k \sigma_{j_{k-1,k+1} \rightarrow j'_{k-1,k+1}}(E_k) \exp(-\beta E_k) dE_k \quad (2)$$

where $\sigma_{j_{k-1,k+1} \rightarrow j'_{k-1,k+1}}(E_k)$ is the rotational transition cross section with $j_{k-1,k+1}$ and $j'_{k-1,k+1}$ being, respectively, the initial and final rotational states of H_2O , m is the reduced mass of the He- H_2O complex, E_k the kinetic energy, and $\beta = (k_B T)^{-1}$, where k_B is Boltzmann's constant.

3. RESULTS AND DISCUSSION

3.1. State-to-state and total deexcitation cross sections

State-to-state deexcitation cross sections were computed for initial rotational levels $1_{1,0}$, $2_{1,2}$, $2_{2,1}$, $3_{0,3}$, $3_{1,2}$, $3_{2,1}$, $4_{1,4}$, $3_{3,0}$, and $4_{2,3}$ of ortho- H_2O and initial levels $1_{1,1}$, $2_{0,2}$, $2_{1,1}$, $2_{2,0}$, $3_{1,3}$, $3_{2,2}$, $4_{0,4}$, $4_{1,3}$, and $3_{3,1}$ of para- H_2O , extending the results from our earlier

work (Yang & Stancil 2007) which was limited to $j \leq 2$. As examples, the state-to-state quenching cross sections from the initial level $3_{0,3}$ of ortho-H₂O and $3_{1,3}$ of para-H₂O are presented in Figs. 1(a) and 1(b), respectively.¹ The agreement between CC and CS calculations, as shown in Fig. 1, is found to be excellent. We conclude that the CS approximation, which is computationally efficient, is reliable for the current collision system at high energies.

From Fig. 1 it can be seen that the cross sections display resonances in the intermediate energy region from 0.1 to 100 cm⁻¹ due to the influence of the attractive part of the interaction potential. The energy location and magnitude of the resonances are sensitive to the details of the PES as shown in Yang & Stancil (2007). Importantly, for astrophysical applications, the properties of the resonances influence the quenching rate coefficients at low temperatures as discussed below. The $3_{0,3} \rightarrow 2_{1,2}$ transition is seen to dominant the quenching of the $3_{0,3}$ level and likewise for para-H₂O, the dominant quenching transition for the $3_{1,3}$ is $3_{1,3} \rightarrow 2_{0,2}$. Both transitions are seen to obey the propensity rule $|\Delta j| = |\Delta k_{+1}| = |\Delta k_{-1}| = 1$.

As a test of the accuracy of our results, we can compare to the recent measurements and calculations of Yang et al. (2010a). In their work, relative DCS measurements of H₂O state-to-state excitation due to He impact were performed at a kinetic energy of 429 cm⁻¹ for 12 different transitions. Differential and integral cross sections were also computed using MOLSCAT, but with the SAPT-H PES. They found good agreement between theory and measurement in all cases except for the $0_{00} \rightarrow 2_{11}$ and $0_{00} \rightarrow 3_{22}$ transitions

¹All state-to-state cross sections and rate coefficients for quenching are available on the UGA Molecular Opacity Project website (www.physast.uga.edu/ugamop/). The rate coefficients are also available in the format of the Leiden Atomic and Molecular Database (LAMDA, Schöier et al. 2005) on our website.

(Yang et al. 2010a). As these transitions are weak (see Fig. 2), the authors argued that the discrepancy may be due to contamination of their beam of ground state molecules (0_{00}) with excited 1_{11} water. For four dominant transitions, the relative DCSs were used to obtain relative integral cross sections which the authors normalized to the largest absolute cross section from their calculations, $0_{00} \rightarrow 1_{11}$. These are reproduced in Fig. 2 adopting the quoted experimental cross section uncertainty of $\pm 30\%$, while the uncertainty in the beam energy was $\pm 20\%$. Also, shown in Fig. 2 and Fig. 3 are the current calculations using the SAPT-P PES, as well as new results using the SAPT-H and VB surfaces, all performed at a kinetic energy of 429 cm^{-1} . As noted in Yang & Stancil (2007), the VB surface gives cross sections that typically differ significantly with results obtained on other surfaces and with available experimental data. This is further confirmed in the present work and with comparison to the Yang et al. (2010a) measurements. For all considered transitions, the current calculations using the SAPT-H and SAPT-P PESs result in similar cross sections. This is consistent with the study performed in Yang & Stancil (2007) which had difficulty in selecting a preferred PES between the two. Significant differences between the current calculations and those of Yang et al. (2010a) are noted, even though both sets of calculations adopted the same surface (SAPT-H) and the same scattering code. For the current calculations, all parameters were carefully checked to ensure convergence and we can offer no explanation for the difference. Finally, the agreement with experiment, regardless of normalization selection, is seen to be excellent for all the calculations for all adopted surfaces (except, of course, for the VB surface). The one exception occurs for the transition $1_{01} \rightarrow 2_{21}$. Yang et al. (2010a) do not comment on this discrepancy and we can only speculate that their beam of 1_{01} molecules may have been contaminated by other low-lying excited states which may have influenced the cross section measurement given its relatively small magnitude. We conclude that the current calculations using the SAPT-P surface gives results of sufficient reliability for astrophysical needs.

State-to-state cross sections from each initial state are summed over all final states to obtain the total deexcitation cross section. In Fig. 4, we compare the total deexcitation cross sections from select initial levels $2_{1,2}$, $3_{1,2}$, and $4_{2,3}$ of ortho-H₂O and $2_{0,2}$, $3_{1,3}$, and $4_{1,3}$ of para-H₂O, while cross sections from some of the lower j levels are given in Yang & Stancil (2007). Generally, the total deexcitation cross sections from different initial levels have similar behavior and are of similar magnitude over the considered energy range. Each of the total cross sections exhibit the behavior predicted by Wigner’s threshold law (Wigner 1948) at ultra-low collision energies, where only s -wave scattering contributes and the cross sections vary inversely with the relative velocity. In the intermediate energy region, between 0.1 and 100 cm⁻¹, the cross sections display scattering resonances. As a consequence of the diverse behavior of the resonances, no trends are evident except at the highest energies where the cross sections increase with rotational excitation.

3.2. State-to-state and total deexcitation rate coefficients

Deexcitation rate coefficients for temperatures ranging from 0.1 to 3000 K are shown in Figs. 5-8 for some select levels of ortho-H₂O and para-H₂O. The rate coefficients are given below 3 K to illustrate their behavior as they approach the zero-temperature limit. Unfortunately, we are unaware of any experimental rate coefficient data for rotational transitions of H₂O due to collisions with He. Therefore, we can only compare our computations with the theoretical results of Green et al. (1993), which were calculated with the potential of Maluendes et al. (1992). The Green et al. (1993) calculations were carried out using MOLSCAT, with the modified log-derivative Airy propagator, and using the CC method for a total energy up to 470 cm⁻¹. For para-H₂O (ortho-H₂) as many as 17 (16) rotational levels were included in their basis. For higher total energies, Green et al. (1993) used the CS approximation up to 5000 cm⁻¹. The primary difference between the current

calculations and those of Green et al. (1993) is the adopted PES.

Figs. 5 and 6, which display state-to-state quenching rate coefficients for ortho-H₂O from initial levels 3_{0,3} and 4_{2,3}, respectively, show that between 0.1 and 50 K, the rate coefficients exhibit an oscillatory temperature dependence due to the presence of resonances. For temperatures above ~ 50 K, the rate coefficients generally increase with increasing temperature. Comparison with the rate coefficients of Green et al. (1993) shows generally good agreement at temperatures above ~ 200 K. The results of Green et al. (1993) are smaller than the present rate coefficients for lower temperatures with the discrepancy increasing with decreasing temperature. The differences are primarily related to the adopted PESs since all other aspects of the two sets of calculations appear to be similar, though different choices of convergence parameters are possible. Further, the bumps in the present rate coefficients are absent from the results of Green et al., likely due to resonances not produced for scattering on the Maluendes et al. (1992) PES.

Considering scattering of para-H₂O by He, the trends noted for ortho-H₂O are also evident in the state-to-state deexcitation rate coefficients as shown in Figs. 7 and 8 for some example initial states. Oscillations due to resonances and a general increase in the rate coefficients above 50 K are similar. Comparisons to the work of Green et al. generally show good agreement, but again only for temperatures above ~ 200 K.

The total deexcitation rate coefficients from all considered initial states (including those given in Yang & Stancil 2007) are shown in Fig. 9. They exhibit similar oscillatory behavior, but the varying oscillation dependencies reflect different resonance energies. For temperatures above ~ 50 K, the total deexcitation rate coefficients smoothly increase with increasing temperature, a trend which may be useful in scaling arguments to estimate rate coefficients for more highly excited states not explicitly computed.

4. ASTROPHYSICAL APPLICATIONS

As discussed in the Introduction, water has been observed in emission and absorption in a variety of astronomical environments. For example, in the past decade there has been increasing interest in the properties of protoplanetary disks (PPDs) and considerable effort has gone into the modeling of PPDs in general and the spectral features of water, in particular (Gorti & Hollenbach 2004; Meijerink et al. 2008, 2009; Glassgold, Meijerink, & Najita 2009; Salyk et al. 2011). The observation of water in PPDs has become very common (Carr & Najita 2008, 2011; Salyk et al. 2011) with interest focused on the inner-planet forming region. Dullemond & Monnier (2010) point out that water is one of dominant coolants in the inner regions.

Because the critical densities of water are typically greater than 10^8 cm^{-3} , models which assume a Boltzmann level population distribution, or local thermodynamic equilibrium (LTE), are generally not valid. Full NLTE models are necessary to predict the rotational and vibrational spectrum of water in most emitting regions of PPDs, above the plane of the disk, as demonstrated by Meijerink et al. (2009) and in a variety of other environments. NLTE models require knowledge of state-to-state rotational (and vibrational) rate coefficients for the kinetic modeling of the internal level populations. Important colliders may include H_2 , H , He , H^+ , and e^- , and for comets H_2O (Bensch & Bergin 2004). A review of the status of collisional rate coefficients for water can be found in van der Tak (2011). Because of the complexity in considering H_2 collisions, there is a long history of initial collisional excitation calculations being performed with He collisions. The He rate coefficients are then often mass-scaled to emulate para- H_2 collisions. We certainly *do not* advocate such a procedure here and it has been pointed out by Dubernet et al. (2009) that mass-scaling does not result in reliable H_2O - H_2 rate coefficients. As a consequence, a considerable amount of effort has been expended to directly compute rate coefficients for rotational excitation of water

by H₂ (Phillips, Maluendes, & Green 1995, 1996; Dubernet & Grosjean 2002; Faure et al. 2006, 2007; Dubernet et al. 2009; Daniel et al. 2010, 2011)², while the rate coefficients for vibrational excitation are limited to the quasi-classical calculations of Faure et al. (2005), with extrapolations proposed by Faure & Josselin (2008). We are unaware of any collisional data for H⁺ impact, we have performed some preliminary calculations for H collisions (Yang & Stancil, in preparation), while Faure & Josselin (2008) have compiled the available electron collision data. However, except for the set of calculations done for temperatures between 20 and 2000 K by Green et al. (1993) on the earlier, and presumably less accurate PES of Maluendes et al. (1992), our previous work (Yang & Stancil 2007), and the small set of calculations in support of the experiments of Yang et al. (2010a,b), no other computations for rate coefficients due to He impact have been published. Therefore, the current rate coefficient calculations, which extend from 10⁻¹ K to 3000 K, are the most comprehensive to date for He and can be utilized in a variety of applications augmenting the datasets developed for H₂ and electrons (see also, the LAMDA website and BASECOL website, Schöier et al. 2005; Dubernet et al. 2006). We note that in NLTE models of water in PPDs, Meijerink et al. (2009) mass-scaled the available H₂O-H₂ rate coefficients to estimate values for H₂O-He.

5. CONCLUSION

Cross sections and rate coefficients for rotational quenching of ortho- and para-H₂O due to He collisions have been studied using the close-coupling method and the coupled-states approximation on the ab initio potential energy surface of Patkowski et al. (2002).

²In particular for H₂O-H₂, the latest state-to-state rate coefficients of Daniel et al. (2011), with a package to calculate effective and thermal rates, can be found on BASECOL.

State-to-state and total deexcitation cross sections and rate coefficients for the first 9 initial excited rotational levels of para- and ortho-H₂O are obtained over a wide temperature range from 0.1 to 3000 K and are available in tables formatted for astrophysical applications. Numerous orbiting resonances result in undulations in the temperature dependence of the rate coefficients. For temperatures less than ~ 200 K, the current state-to-state rotational rate coefficients are found to depart from the results of Green et al. (1993) obtained with the earlier PES of Maluendes et al. (1992). Discrepancies are primarily related to differences in the adopted PESs as all other aspects of the current calculations are similar to those of Green et al. (1993).

We dedicate this manuscript to the memory of Professor Mineo Kimura who passed away during the completion of the work presented here. B.H.Y. and P.C.S. acknowledge support from NASA under Grants No. NNX07AP12G and NNX12AF42G.

REFERENCES

- Alexander, M. H., & Manolopoulos, D. E. 1987, *J. Chem. Phys.*, 86, 2044
- Aquillanti, V., Cornicchi, E., Teixidor, M. M., Saendig, N., Pirani, F., & Cappelletti, D. 2005, *Angew. Chem. Int. Ed.*, 44, 2356
- Barman, T. S. 2008, *ApJ*, 676, L61
- Bensch, F. & Bergin, E. A. 2004, *ApJ*, 615, 531
- Bickes, Jr., R. W., Duquette, G., van den Meijdenberg, C. J. N., Rulis, A. M., Scoles, G., & Smith, K. M. 1975, *J. Phys. B*, 8, 3034
- Brudermann, J., Steinbach, C., Buck, U., Patkowski, K., & Moszynski, R. 2002, *J. Chem. Phys.*, 117, 11166
- Calderoni, G., Cargnoni, F., & Raimondi, M. 2003, *Chem. Phys. Lett.*, 370, 233
- Cappelletti, D., Aquillanti, V., Cornicchi, E., Teixidor, M. M., & Pirani, F. 2005, *J. Chem. Phys.*, 123, 024302
- Carr, J. S. & Najita, J. R. 2008, *Science*, 319, 1504
- Carr, J. S. & Najita, J. R. 2011, *ApJ*, 733, 102
- Caselli, P., Keto, E., & Pagani, L., et al. 2011, *A&A*, 521, L29
- Chavarria, L., et al. 2010, *A&A*, 521, L37
- Dagdigian, P. J & Alexander, M. 2010, *Mol. Phys.*, 108, 1159
- Daniel, F., Dubernet, M.-L., Pacaud, F., & Grosjean, A. 2010, *A&A*, 517, A13
- Daniel, F., Dubernet, M.-L., & Grosjean, A. 2011, *A&A*, 536, A76

- Dick, M. J., Drouin, B. J., & Pearson, J. C. 2010, *Phys. Rev. A*, 81, 022706
- Doty, S. D. & Neufeld, D. A. 1997, *ApJ*, 489, 122
- Dubernet, M. L., Grosjean, A., Daniel, F., et al. 2006, *Journal of Plasma and Fusion Research SERIES*, 7, 356-357
- Dubernet, M.-L., Daniel, F., Grosjean, A., & Lin, C. Y. 2009, *A&A*, 497, 911
- Dubernet, M.-L. & Grosjean, A. 2002, *A&A*, 390, 793
- Dullemond, C. P. & Monnier, J. D. 2010, *ARA&A*, 48, 205
- Ehrenreich, D., Hébrard, G., Lecavelier des Etangs, A., et al., 2007, *ApJ*, 668, L179
- Faure, A., Crimier, N., Ceccarelli, C., Valiron, P., Wiesenfeld, L., & Dubernet, M.-L. 2007, *A&A*, 472, 1029
- Faure, A. & Josselin, E. 2008, *A&A*, 492, 257
- Faure, A., Valiron, P., Wernli, M., et al. 2005, *J. Chem. Phys.*, 122, 221102
- Faure, A., Wiesenfeld, L., Wernli, M., & Valiron, P. 2006, *J. Chem. Phys.*, 124, 214310
- Flower, D. R. 2007, *Molecular Collisions in the Interstellar Medium*, 2nd ed. (Cambridge Univ. Press)
- Flower, D. R. & Pineau des Forêts, G. 2010, *MNRAS*, 406, 1745
- Franklin, J., Snell, R. L., Kaufman, M. J., et al., 2008, *ApJ*, 674, 1015
- Garrison, B. J., Lester, Jr., W. A., & Miller, W. H. 1976, *J. Chem. Phys.*, 65, 2193
- Glassgold, A. E., Meijerink, R., & Najita, J. R. 2009, *ApJ*, 701, 142
- Gorti, U. & Hollenbach, D. 2004, *ApJ*, 613, 424

- Green, S. 1976, *J. Chem. Phys.*, 64, 3463
- Green, S. 1980, *ApJS*, 42, 103
- Green, S. 1989, *ApJS*, 70, 813
- Green, S., DeFrees, D. J., & McLean, A. D. 1991, *J. Chem. Phys.*, 94, 1346
- Green, S., Maluendes, S., & McLean, A., D. 1993, *ApJS*, 85, 181
- Grillmair, C. J., Burrows, A., Charbonneau, D., et al. 2008, *Nature*, 456, 767
- Hodges, M. P., Wheatley, R. J. & Harvey, A. H. 2002, *J. Chem. Phys.*, 116, 1397
- Hutson, J. M., & Green, S. 1994, MOLSCAT computer code, version 14, Collaborative Computational Project No. 6 of the Engineering and Physical Sciences Research Council (UK)
- Kukawska-Tarnawska, B., Chalasinski, G., & Szczesniak, M. M. 1993, *J. Mol. Struct.*, 297, 313
- Kyrö, E. 1981, *J. Mol. Spectrosc.*, 88, 167
- Lanquetin, R., Coudert, L. H., & Camy-Peyret, C. 1999, *J. Mol. Spectrosc.*, 195, 54
- Makarewicz, J., 2008, *J. Chem. Phys.* 129, 184310
- Maluendes, S., McLean, A. D., & Green, S. 1992, *J. Chem. Phys.*, 96, 8150
- Meijerink, R., Poelman, D. R., Spaans, M., Tielens, A. G. G. M., & Glassgold, A. E. 2008, *ApJ*, 689, L57
- Meijerink, R., Pontoppidan, K. M., Blake, G. A., Poelman, D. R., & Dullemond, C. P. 2009, *ApJ*, 704, 1471

- Melnick, G. J., Tolls, V., Neufeld, D. A., et al. 2008, *ApJ*, 683, 876
- Neufeld, D. A., Bergin, E. A., Melnick, G. J., & Goldsmith, P. F. 2003, *ApJ*, 590, 882
- Palma, A., Green, S., DeFrees, D. J., & McLean, A. D. 1988a, *J. Chem. Phys.*, 89, 1401
- Palma, A., Green, S., DeFrees, D. J., & McLean, A. D. 1988b, *ApJS*, 68, 287
- Patkowski, K., Korona, T., Moszynski, R., Jeziorski, B., & Szalewic, K. 2002, *J. Mol. Struct. : THEOCHEM*, 591, 231
- Phillips, T. R., Maluendes, S., & Green, S. 1995, *J. Chem. Phys.*, 102, 6024
- Phillips, T. R., Maluendes, S., & Green, S. 1996, *ApJS*, 107, 467
- Salyk, C., Pontoppidan, K. M., Blake, G. A., Najita, J. R., & Carr, J. S. 2011, *ApJ*, 731, 130
- Schöier, F. L., van der Tak, F. F. S., van Dishoeck, E. F., & Black, J. H. 2005, *A&A*, 432, 369
- Slankas, J. T., Keil, M., & Kuppermann, A. 1979, *J. Chem. Phys.*, 70, 1482
- Tao, F. M., Li, Z., & Pan, Y. K. 1996, *Chem. Phys. Lett.*, 255, 179
- Valiron, P., Wernli, M., Faure, A., et al. 2008, *J. Chem. Phys.*, 129, 134306
- van der Tak, F. 2011, from *The Molecular Universe*, Proc. IAU Symp. 280, ed. J. Cernicharo & R. Bachiller
- van Dishoeck, E. F., Kristensen, L. E., & Benz, A. O., et al. 2011, *PASP*, 123, 138
- Wigner, E. P. 1948, *Phys. Rev.*, 73, 1002
- Whittet, D. C. B., Gerakines, P. A., Hough, J. H., & Shenoy, S. S., 2001, *ApJ*, 547, 872

- Wright, C. M., van Dishoeck, E. F., Black, J. H., Feuchtgruber, H., Cernicharo, J., Gonzalez-Alfonso, E., de Graauw, Th. 2000, *A & A*, 358, 689
- Yang, B. H., & Stancil, P. C. 2007, *J. Chem. Phys.*, 126, 154306
- Yang, C.-H., Sarma, G., ter Meulen, J. J., Parker, D. H., Buck, U., & Wiesenfeld, L. 2010a, *J. Phys. Chem. A*, 114, 9886
- Yang, C.-H., Sarma, G., ter Meulen, J. J., Parker, D. H., McBane, G. C., Wiesenfeld, L., Faure, A., Scribano, Y., & Feautrier, N. 2010b, *J. Chem. Phys.*, 133, 131103

Table 1: Rotational energy levels (cm^{-1}) of ortho- and para- H_2O

ortho- H_2O		para- H_2O	
$1_{0,1}$	23.7943	$0_{0,0}$	0.0000
$1_{1,0}$	42.3717	$1_{1,1}$	37.1371
$2_{1,2}$	79.4963	$2_{0,2}$	70.0907
$2_{2,1}$	134.9018	$2_{1,1}$	95.1757
$3_{0,3}$	136.7617	$2_{2,0}$	136.1641
$3_{1,2}$	173.3656	$3_{1,3}$	142.2783
$3_{2,1}$	212.1561	$3_{2,2}$	206.3013
$4_{1,4}$	224.8383	$4_{0,4}$	222.0529
$3_{3,0}$	285.4192	$4_{1,3}$	275.4971
$4_{2,3}$	300.3621	$3_{3,1}$	285.2200
$5_{0,5}$	325.3483	$4_{2,2}$	315.7792
$4_{3,2}$	382.5171	$5_{1,5}$	326.6256

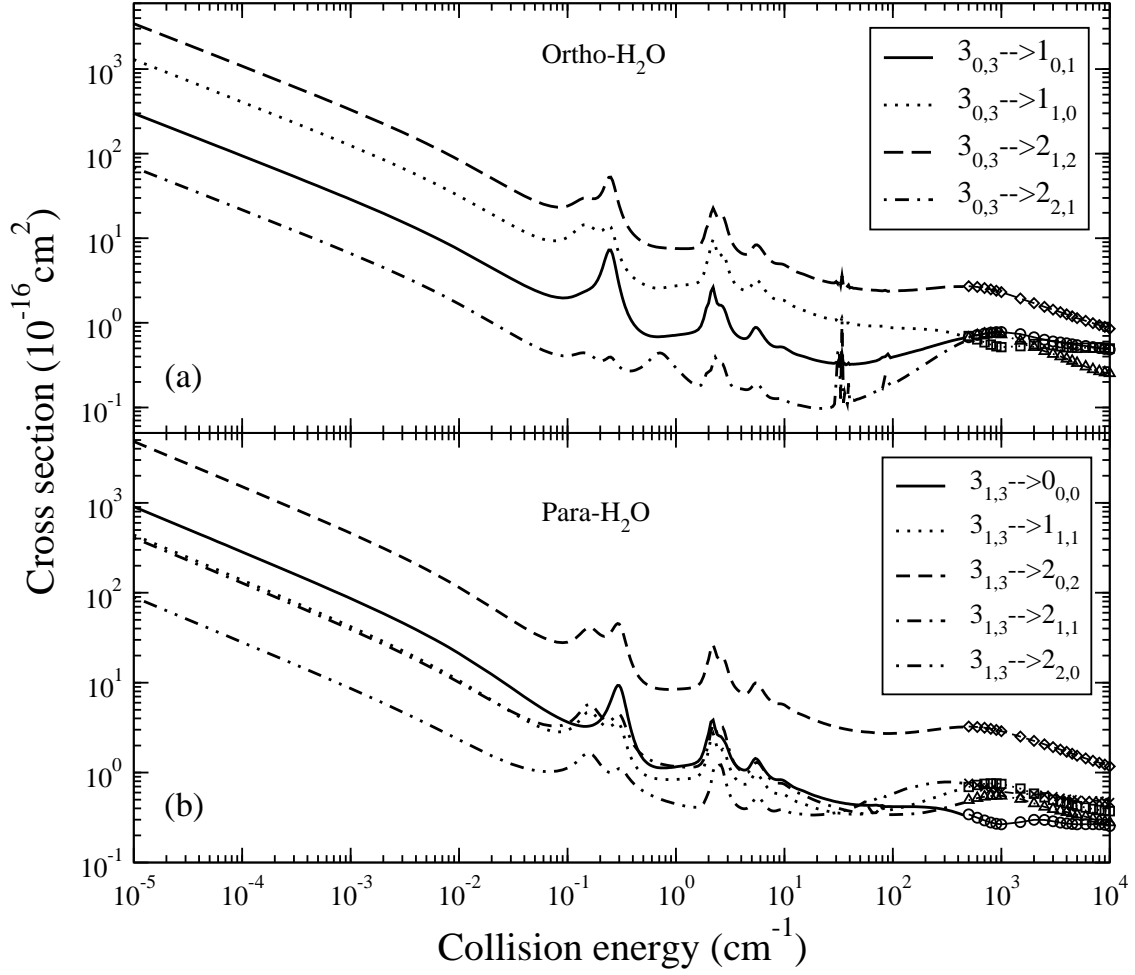


Fig. 1.— State-to-state deexcitation cross sections of H₂O in collisions with He as a function of kinetic energy obtained with the CC method (lines) and the CC approximation (symbols). (a) $3_{0,3}$ of ortho-H₂O, (b) $3_{1,3}$ of para-H₂O.

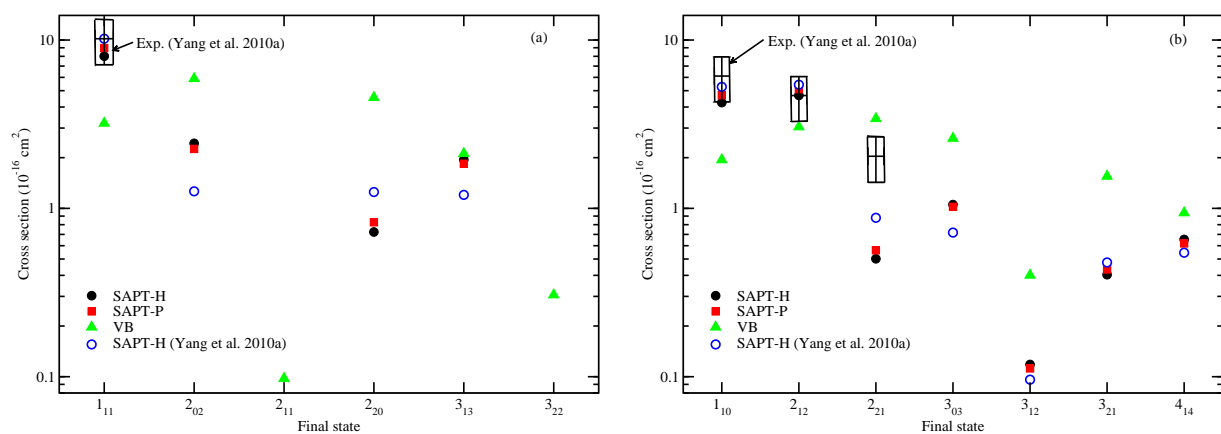


Fig. 2.— Comparison of state-to-state H_2O -He excitation cross sections at 429 cm^{-1} from the initial states (a) 0_{00} and (b) 1_{01} . Open circle, CC calculations of Yang et al. (2010a); filled symbols, current CC calculations; boxes, experiment of Yang et al. (2010a). Note that in (a) the cross section magnitudes from other calculations to the 2_{11} and 3_{22} are smaller than the scale of the plot.

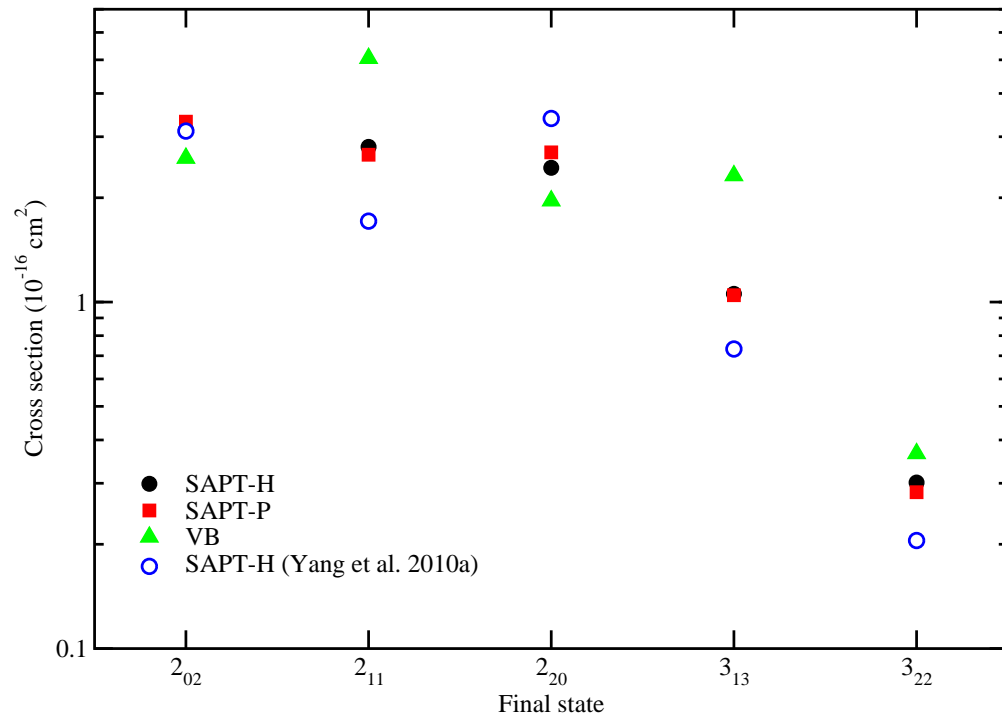


Fig. 3.— Same as Fig. 2, but for the initial state 1_{11} . No experimental integral cross sections are available for this state.

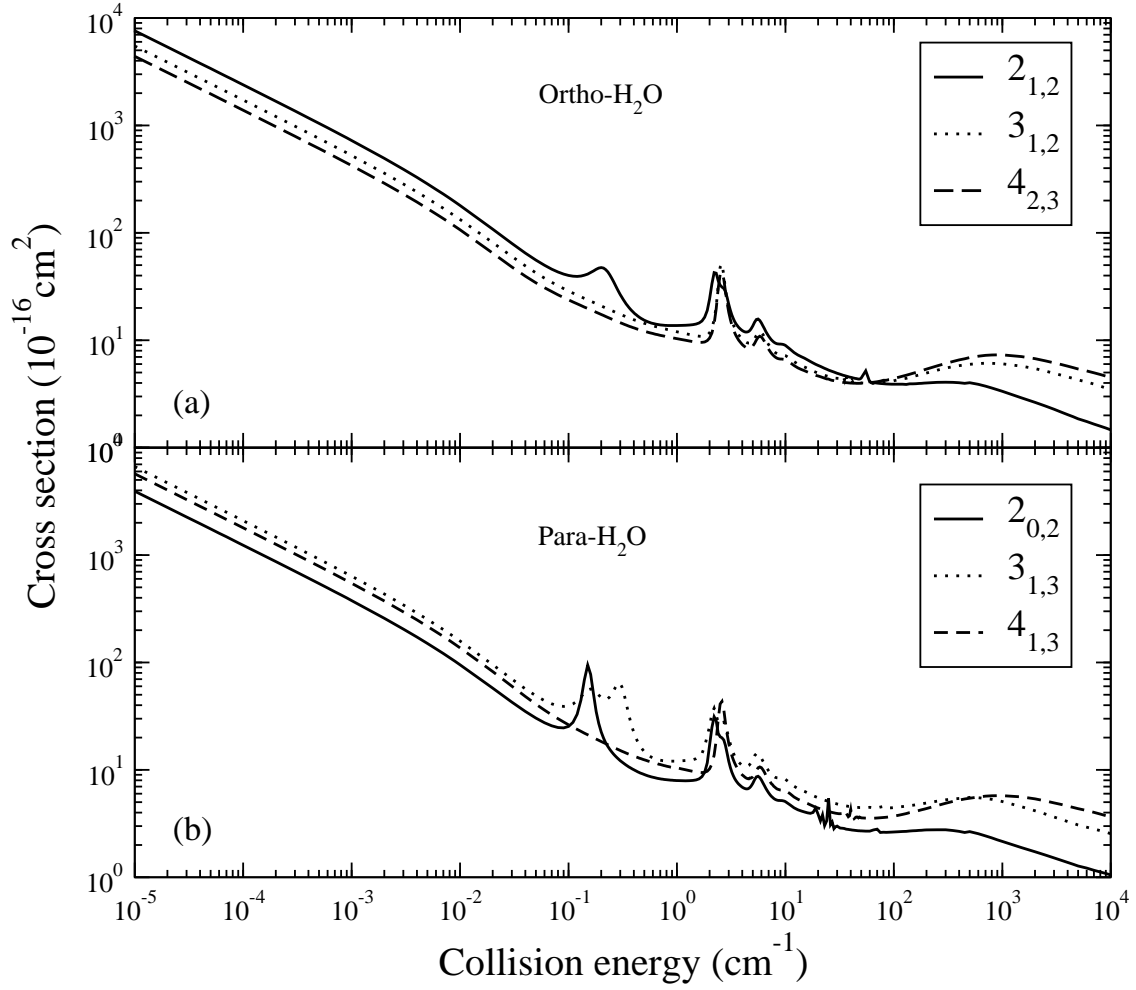


Fig. 4.— Total deexcitation cross sections from states: (a) $2_{1,2}$, $3_{1,2}$, and $4_{2,3}$ of ortho- H_2O , and (b) $2_{0,2}$, $3_{1,3}$, and $4_{1,3}$ of para- H_2O in collisions with He as a function of kinetic energy.

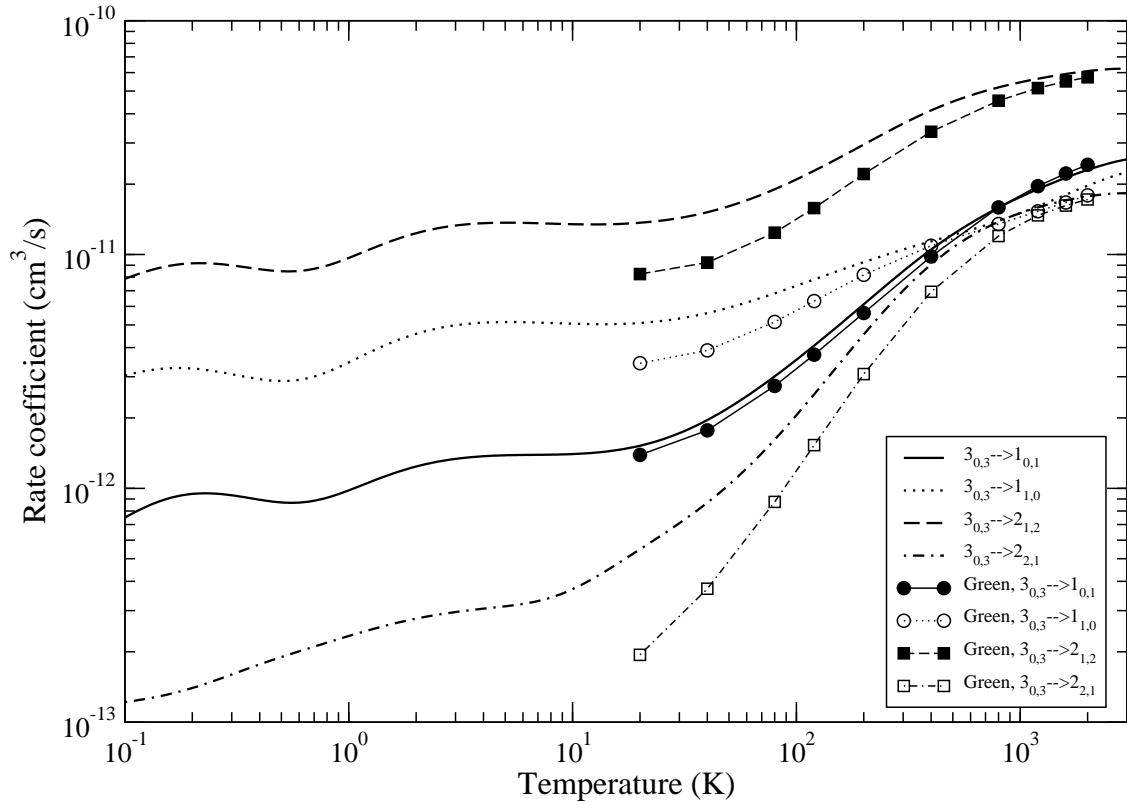


Fig. 5.— The state-to-state deexcitation rate coefficients from initial state $3_{0,3}$ of ortho- H_2O by collisions with He atoms as a function of temperature. Current results (lines) and results from Green et al. (1993) (symbols with lines).

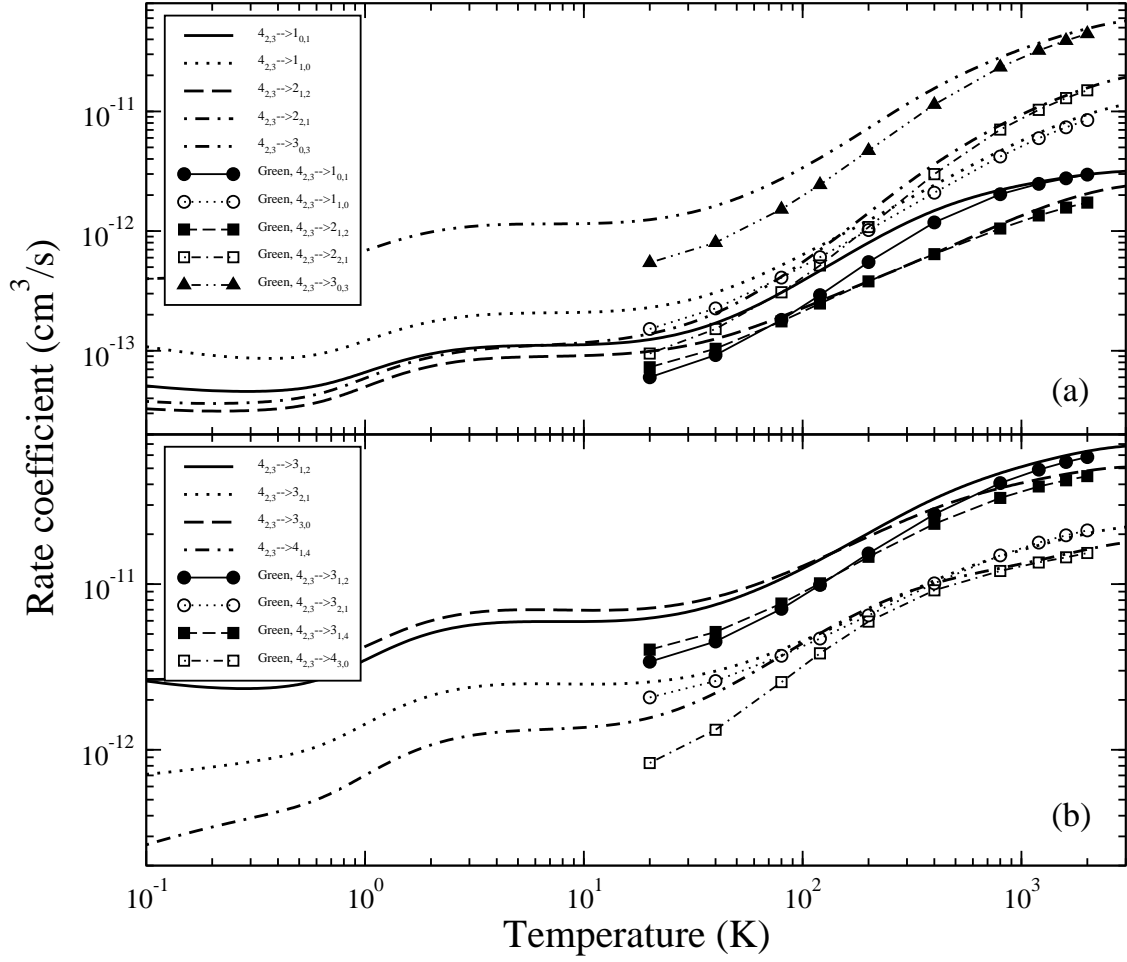


Fig. 6.— Same as Fig. 5, but for ortho- H_2O initial state $4_{2,3}$.

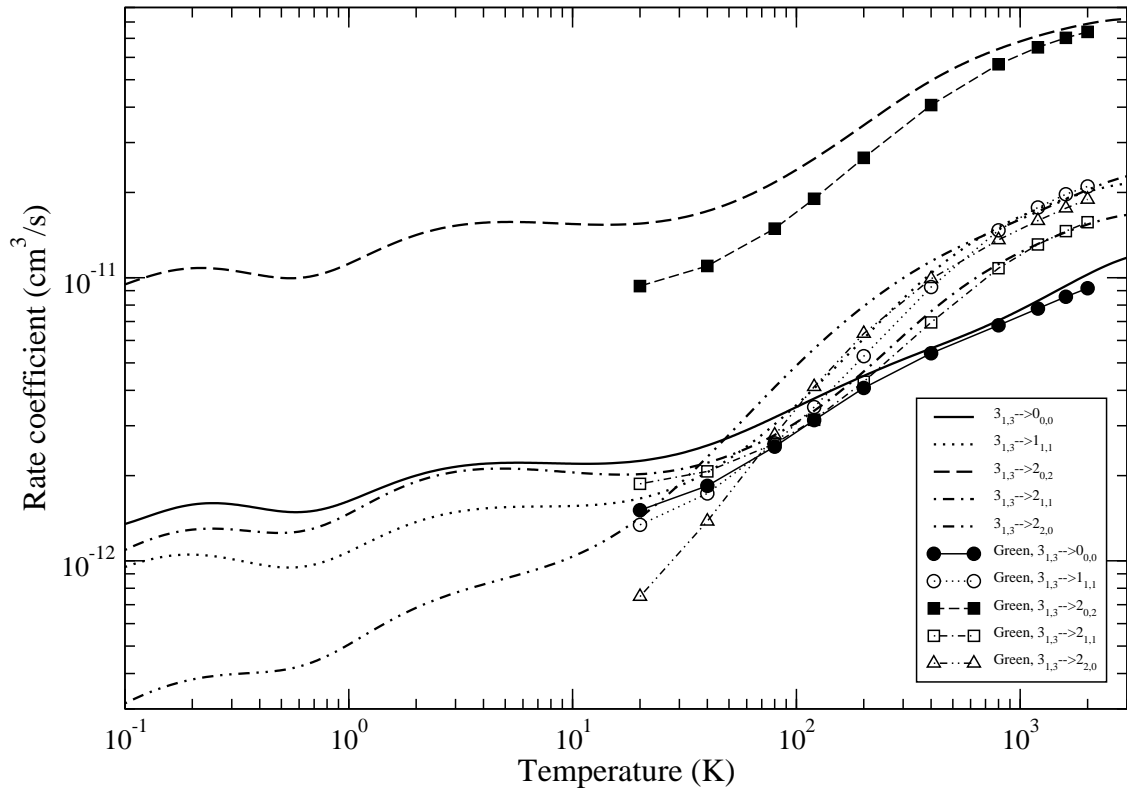


Fig. 7.— Same as Fig. 5, but for para- H_2O initial state $3_{1,3}$.

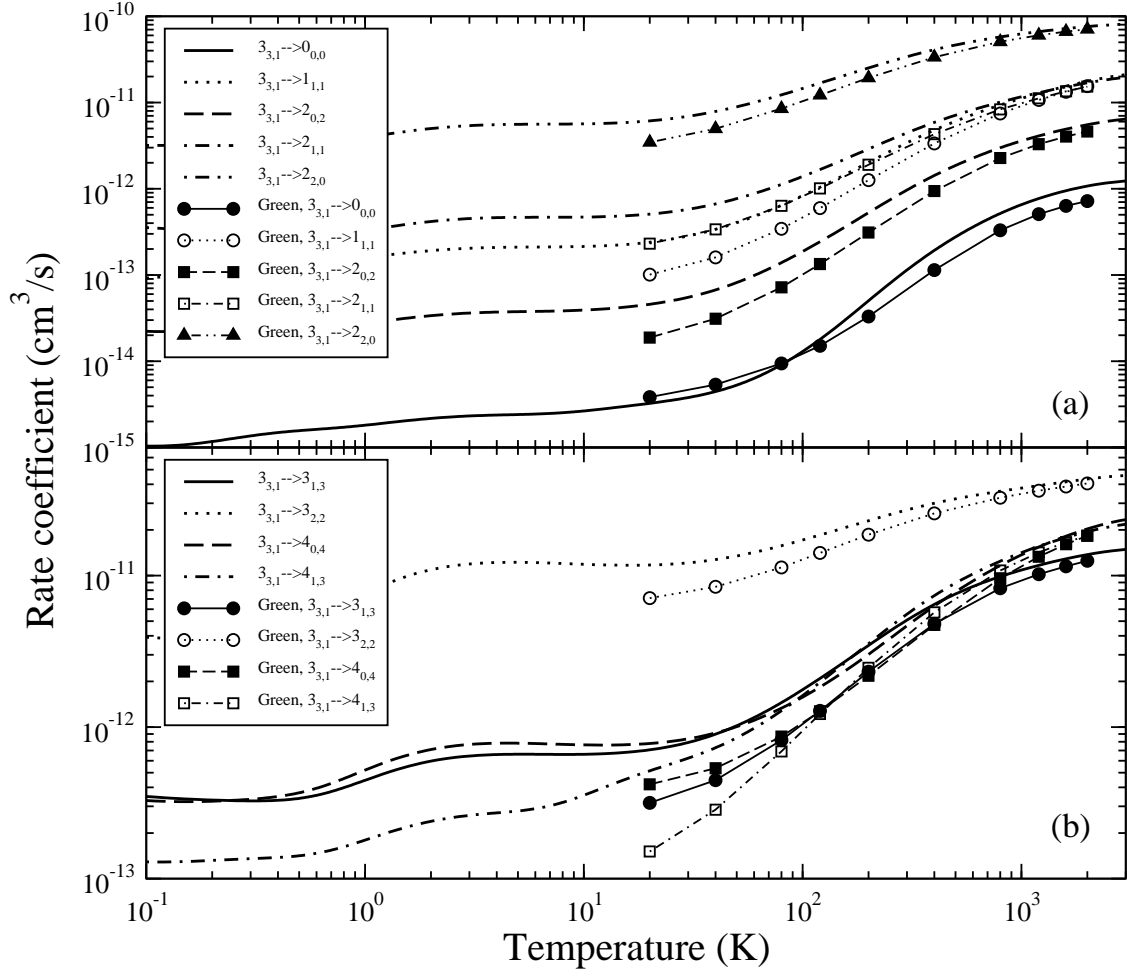


Fig. 8.— Same as Fig. 5, but for para- H_2O initial state $3_{3,1}$.

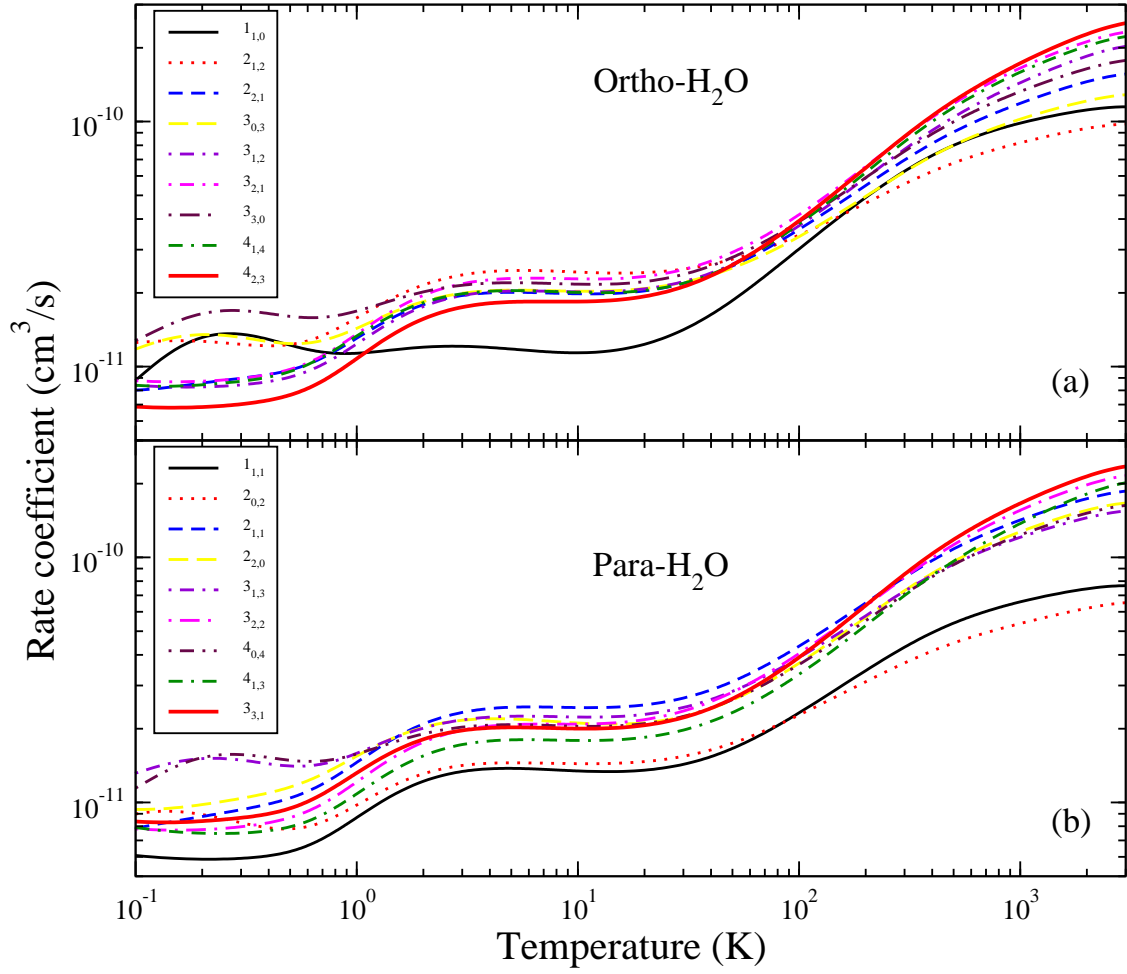


Fig. 9.— The total H₂O-He excitation rate coefficients as a function of temperature. (a) Ortho-H₂O, (b) para-H₂O.